

Structure, Volume 24

Supplemental Information

**The Structure of HIV-1 Rev Filaments Suggests
a Bilateral Model for Rev-RRE Assembly**

Michael A. DiMattia, Norman R. Watts, Naiqian Cheng, Rick Huang, J. Bernard Heymann, Jonathan M. Grimes, Paul T. Wingfield, David I. Stuart, and Alasdair C. Steven

Supplemental Information

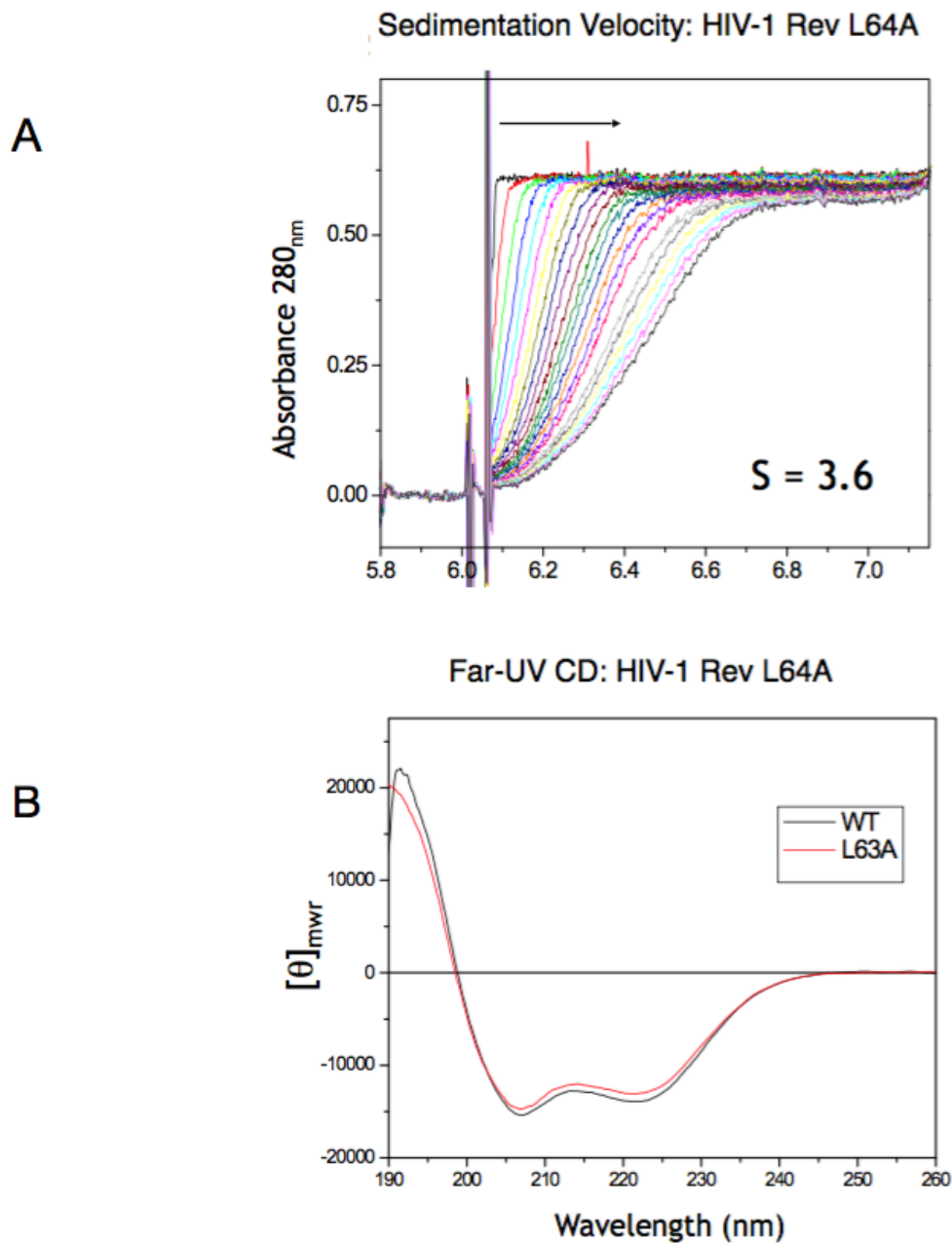


Fig. S1 Sedimentation Velocity and circular dichroism analysis of Rev A-A interface mutant, related to Fig. 2. (A) Overlaid absorbance scans at 280 nm vs radial positions are shown for Rev L64A. The arrow indicates the direction of sedimentation. These data were used to calculate sedimentation coefficients (s) using DCDT+. The data indicate a sedimentation coefficient of 3.6 for Rev L64A and an estimated mass of 47 kDa, corresponding to an approximately trimeric association. (B) The far UV spectra shown for WT and L64A mutant have typical helical signatures.

Rev

Rev L64A

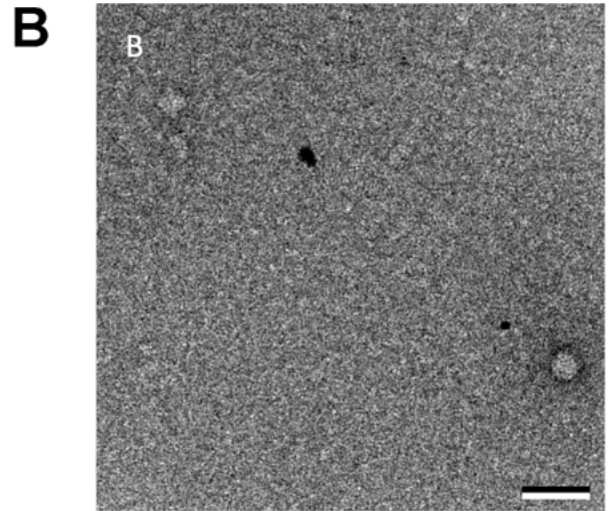
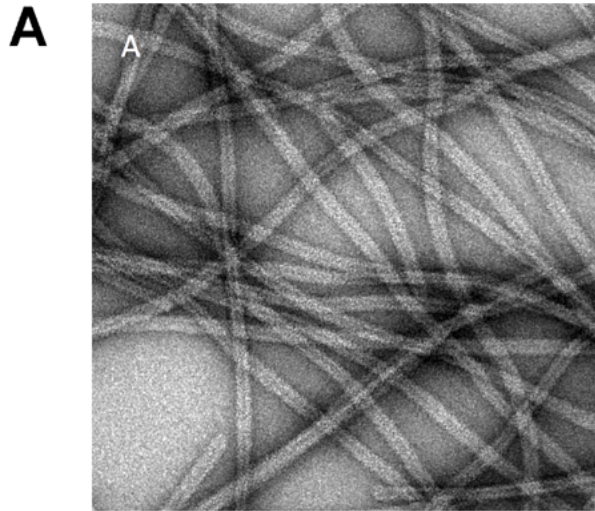


Fig. S2 Negative stain electron microscopy of Rev A-A interface mutants, related to Fig. 2.

Shown are images of folded and polymerized Rev proteins as visualized by negative stain electron microscopy. (A) Rev wild-type, (B) Rev L64A. The protein concentration of the sample applied to grids was 0.2 mg/ml, above the threshold concentration at which wild type Rev filaments readily fold. Scale bar = 50 nm.

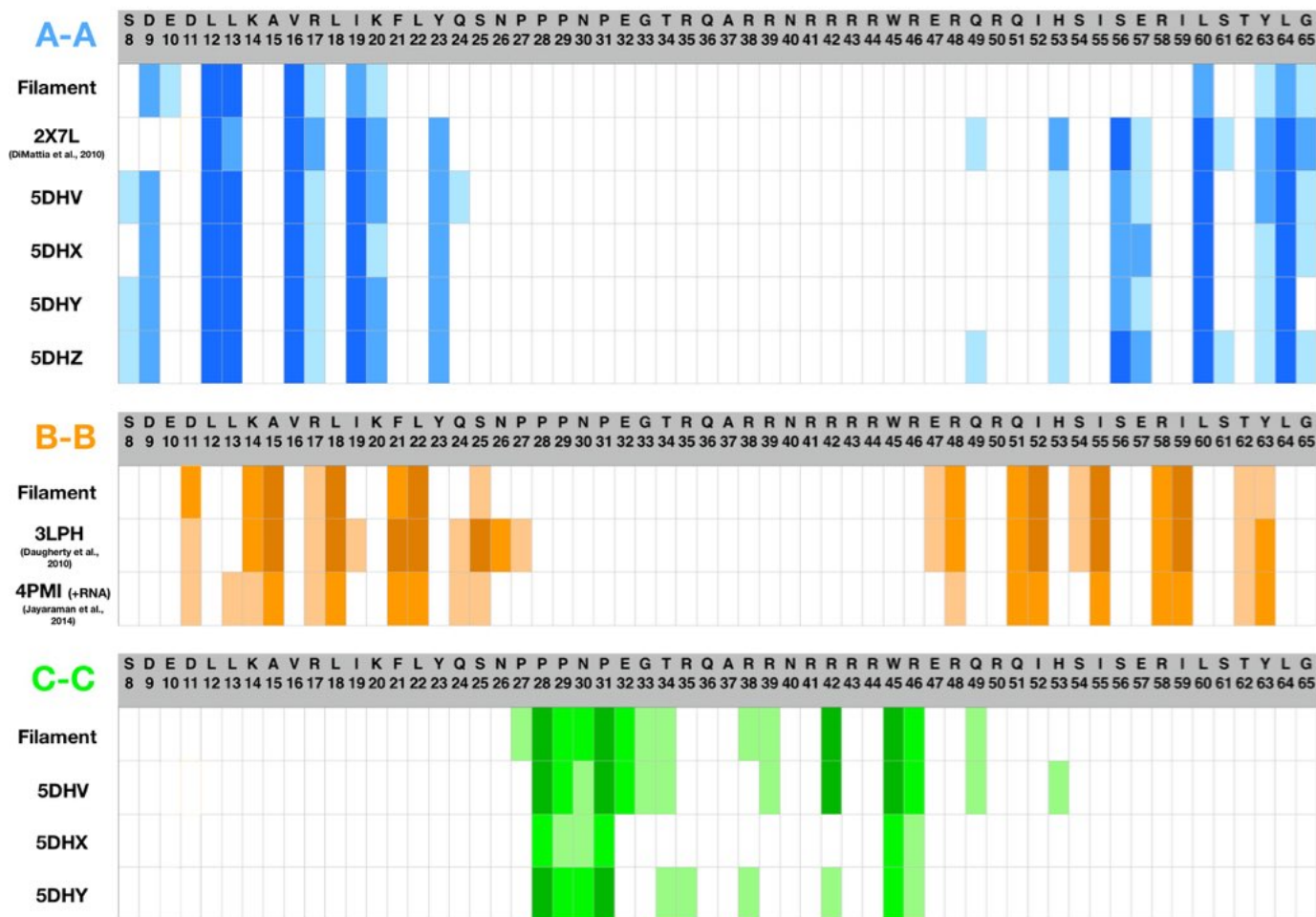


Fig. S3 Rev-Rev interface summary, related to Fig. 2. Shown above are three tables, one for each Rev oligomerization interface, A-A (blue), B-B (orange), and C-C (green). One column has been assigned to each Rev NTD residue (from 8-65). Represented visually is the buried surface area of each residue, calculated as a fraction of the total solvent-accessible surface area of that residue (when not interacting) that is buried upon interface formation. White = 0% BSA, light = 10-30%, medium = 40-60%, dark = 70-100%. Each row corresponds to a different Rev dimer structure. Filament = Rev dimer structure fitted into 8.3-Å res. map of Rev filaments. References for PDB IDs 2X7L, 3LPH, and 4PMI are DiMattia et al., 2010; Daugherty et al., 2010; and Jayaraman et al., 2014. Note the apparent similarity between the A-A, B-B, and C-C interfaces as they occur in the filament vs. those in the crystal structures.

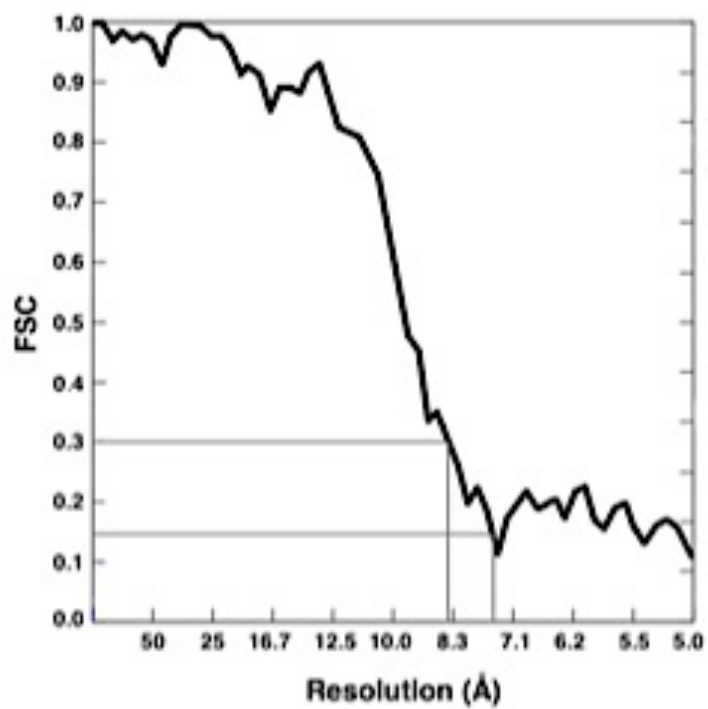


Fig. S4 Fourier Shell Correlation Plot, related to Fig. 1. Resolution is assessed to be 8.3 Å (at FSC value of 0.3).

Sedimentation Velocity: Rev C-C interface mutants

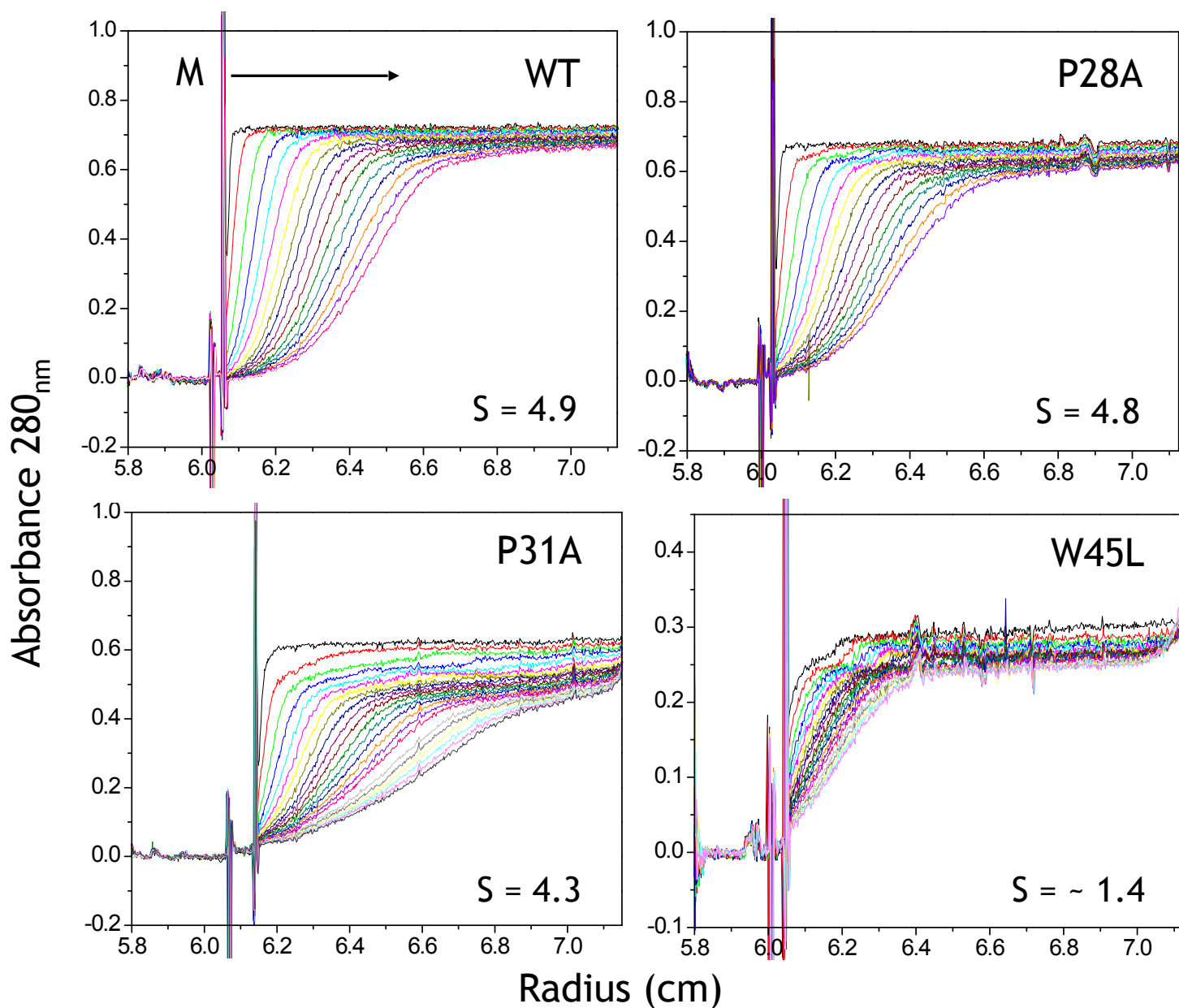


Fig. S5 Sedimentation Velocity analysis of Rev C-C interface mutants, related to Fig. 3. Overlaid absorbance scans at 280 nm vs radial positions are shown for HIV-1 Rev and the three mutants. M indicates the solvent meniscus and the arrow the direction of sedimentation. These data were used to calculate sedimentation coefficients (s) using DCDT+.

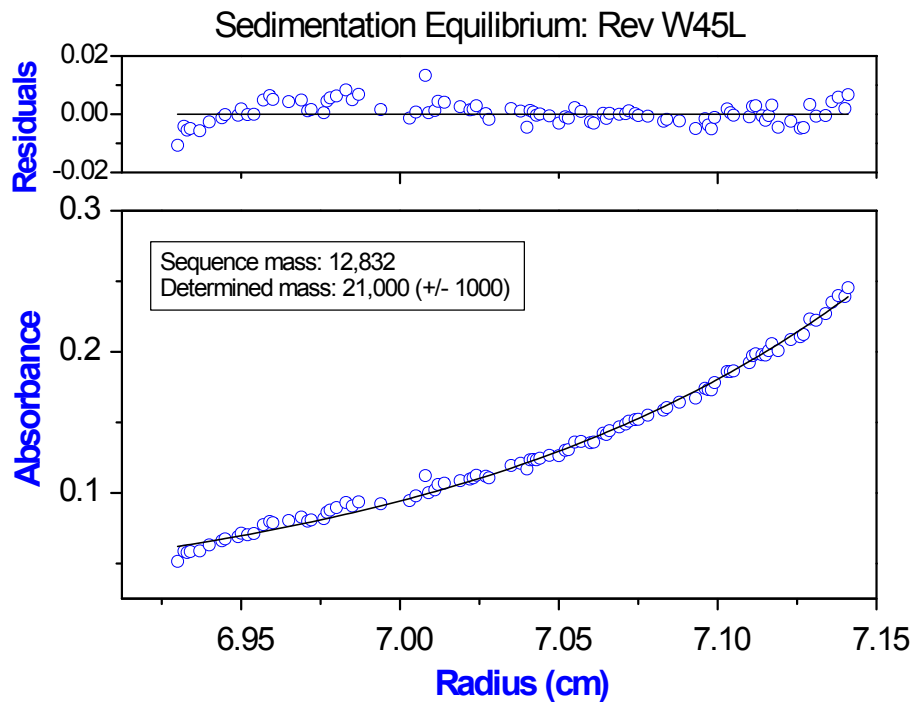


Fig. S6 Sedimentation Equilibrium analysis of Rev W45L, related to Fig. 3. Open circles show the protein concentration profile represented by the UV absorbance gradient in the centrifuge cell at 280 nm. The solid line indicates the calculated fit for a single ideal species. Residuals in the top panel show the difference between the fitted and experimental values as a function of radial position.

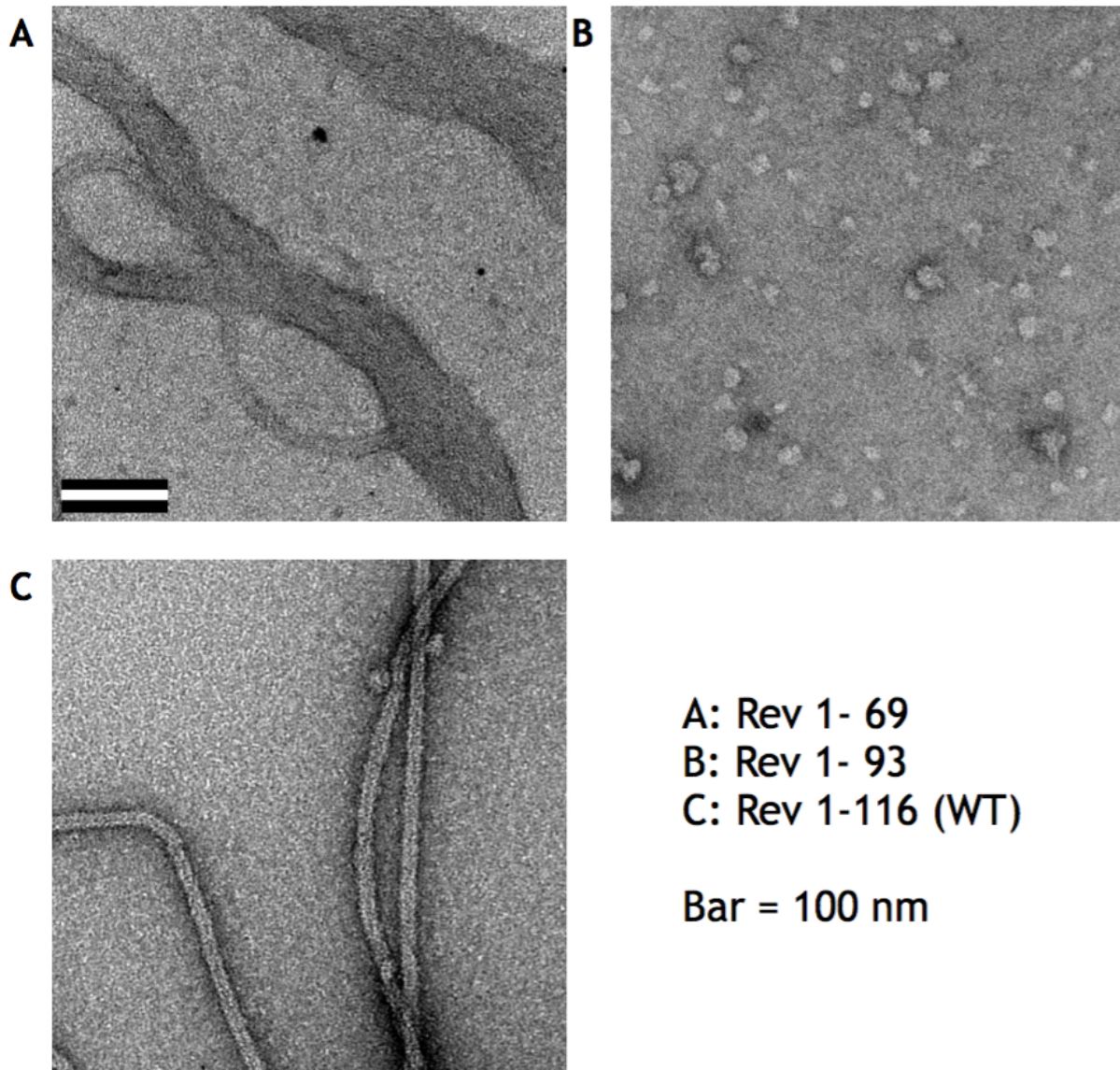


Fig. S7 Rev 1-69 and Rev 1-93 do not form filaments *in vitro*, related to Fig. 8. Representative negative-stain electron micrograph of (A) Rev NTD (residues 1-69), (B) Rev 1-93 and (C) Rev WT. No recognizable Rev filaments were observed in (A) or (B), suggesting that the CTD (residues 70-116) is necessary for *in vitro* filament formation. In connection with this idea, we observe partial ordering of the CTD on the exterior surface of Rev filaments in cryo-EM helical reconstructions (see Fig. 7). Consistent with these observations is previously reported negative stain EM of Rev filaments that are labelled on the exterior surface with Fab antibody fragments whose epitope is the Rev C-terminus (residues 96-116) (Zhuang et al., 2014).